Supporting Information

for

Minor difference in the hydrogen-bonding group structure has a major impact on the mechanical properties of polymers

Authors:

Shogo Ishizaka, Shintaro Nakagawa, and Naoko Yoshie*

* Corresponding author, E-mail: yoshie@iis.u-tokyo.ac.jp

Affiliations:

Institute of Industrial Science, The University of Tokyo, Komaba 4-6-1, Meguro-ku, Tokyo, 153-8505, Japan

Table of contents

1. Experimental

Materials

Grubbs 3rd generation catalyst (G3) (Sigma Aldrich, USA), dichloromethane (DCM) (Wako, Japan), ethyl vinyl ether (Wako, Japan), methanol (MeOH) (Wako, Japan), 2,6-di-*tert*-butyl-4-methylphenol (BHT) (Wako, Japan), tetrahydrofuran (THF) (Wako, Japan) and 6 M hydrochloric acid (HClaq) (Wako, Japan) were used as received. 2,2-di((*tert*-butyldimethylsilyloxy)methyl)-5-norbornene ((2,2)DiOTBS)[1], 2-*endo*,3-*endo*-di((*tert*-butyldimethylsilyloxy)methyl)-5-norbornene ((2,3)DiOTBS)[2], dodecyl 5-norbornene-2-carboxylate (Dodec)[3], and (2,3)DiOTBS-*x* (*x* = 120, 160, and 200)[4] were synthesized according to the literatures. The ^{1}H NMR spectrum of synthesized (2,2)DiOTBS are shown in **Figure S2**. The ^{1}H NMR spectrum, the SEC profiles, and the IR spectra of the copolymers containing (2,3)DiOTBS, i.e., (2,3)DiOTBS-*x* (*x* = 120, 160, and 200), are shown in **Figure S19-S25**.

Synthesis of (2,2)DiOTBS-200

G3 7.99 mg (9.03 μmol, 1 eq.) was weighed in a 50 mL glass vial equipped with a rubber septum. This vial was cooled in an ice bath and purged with nitrogen gas. DCM 30 mL was added through the septum to dissolve the catalyst. A 10 mL syringe was loaded a solution of (2,2)DiOTBS 692.23 mg (1.81 mmol, 200 eq.) in DCM 5 mL. After the syringe was placed in the syringe pump, the solution with (2,2)DiOTBS was pumped at 2.0 mL/h and injected with vigorous stirring. Another 10 mL syringe was loaded a solution of Dodec 554.32 mg (1.81 mmol, 200 eq.) in DCM 5 mL. After the syringe was placed in the syringe pump, the solution with Dodec was pumped at 1.5 mL/h (for 0.5 h), 2.0 mL/h (for 2 h), and 0.5 mL/h (for 0.5 h), respectively, and injected with vigorous stirring. After stirring for 3 h, the polymerization was quenched by adding a few drops of ethyl vinyl ether followed by stirring for 30 min at room temperature. Precipitation in cold MeOH containing BHT and dying under reduced pressure for 3 h at 40 °C yielded (2,2)DiOTBS-200 as a pale brown sticky solid. Yield: 1030.57 mg (82.7%). For copolymerization analysis, the reaction mixture (0.5 mL) was extracted at seven different time points (0.5, 1.0, 1.5, 2.0, 2.5, and 3.0 h). The ^{1}H NMR spectra of the reaction mixture and the product are shown in **Figure S7** and **S16**, respectively. The SEC profiles of the reaction mixture and the product are shown in **Figure S8** and **S25**, respectively.

Synthesis of (2,2)DiOTBS-160

The procedure was the same as (2,2)DiOTBS-200. The used substances are as follows: G3 8.00 mg (9.04 μmol, 1 eq.), (2,2)DiOTBS 553.80 mg (1.45 mmol, 160 eq.), Dodec 665.26 mg (2.17 mmol, 240 eq.), and DCM 35 mL in a 50 mL glass vial. Yield: 968.28 mg (79.4%). The ^{1}H NMR spectra of the reaction mixture and the product are shown in **Figure S6** and **S13**, respectively. The SEC profiles of the reaction mixture and the product are shown in **Figure S8** and **S25**, respectively.

Synthesis of (2,2)DiOTBS-120

The procedure was the same as (2,2)DiOTBS-200. The used substances are as follows: G3 8.00 mg (9.04 μmol, 1 eq.), (2,2)DiOTBS 415.40 mg (1.09 mmol, 120 eq.), Dodec 665.26 mg (2.53 mmol, 280 eq.), and DCM 40 mL in a 50 mL glass vial. Yield: 941.23 mg (79.0%). The ^{1}H NMR spectra of the reaction mixture and the product are shown in **Figure S5** and **S10**, respectively. The SEC profiles of the reaction mixture and the product are shown in **Figure S8** and **S25**, respectively.

General procedure for the synthesis of (2,2)Diol-x

The procedure for (2,2)Diol-120 is described as an example. To a solution of (2,2)DiOTBS-120 901.26 mg in THF 30 mL, HClaq 2.40 mL (14.5 mmol) was added. After stirring overnight, precipitation in cold 9:1 mixture of MeOH and water containing BHT and drying under reduced pressure for 3 h at 60 °C. The obtained polymer was again dissolved in THF 30 mL, HClaq 2.40 mL (14.5 mmol) was added, and the mixture was stirred overnight. (2,2)Diol-120 was obtained as a pale brown rubbery solid by reprecipitation and drying in the same procedure. Yield: 641.37 mg (90.0%). The ^{1}H NMR spectra of the product are shown in **Figure S11**, **S14**, and **S17**. The IR spectra of the products are shown in **Figure S12**, **S15**, and **S18**.

General procedure for the synthesis of (2,3)Diol-x

The procedure for (2,3)Diol-120 is described as an example. To a solution of (2,3)DiOTBS-120 872.49 mg in THF 30 mL, HClaq 2.40 mL (14.5 mmol) was added. After stirring for 240 min, precipitation in cold 9:1 mixture of MeOH and water containing BHT and drying under reduced pressure for 3 h at 60 °C yielded (2,3)Diol-120 as a pale brown rubbery solid. Yield: 636.12 mg (92.1%). The IR spectra of the products are shown in **Figure S20**, **S22**, and **S24**.

Sample preparation

Sample films with small-angle X-ray scattering (SAXS), dynamic mechanical analysis (DMA), and tensile tests were prepared by hot-pressing the polymer between Teflon® sheets separated by a stainless-steel spacer with each thickness at 80 °C and 10 MPa for 10 min, with the same procedure as the literature[5].

^{1}H NMR, SEC, and IR characterization

^{1}H NMR spectra were recorded on a JNM-AL 400 (JEOL, Japan) or an JNM-ECZ 600R (JEOL, Japan) in $CDCl_3$. The solvent signal at 7.26 ppm was used as an internal standard. Size exclusion chromatography (SEC) was performed on an SEC system equipped with a ResiPore column (Agilent, USA) and a refractive index detector (RID-20A, Shimadzu, Japan), with the same procedure as the literature[5]. Chloroform was used as the eluent. Polystyrene standards were used as a calibrant. Infrared (IR) spectra were recorded on an IRAffinity-1S (Shimadzu, Japan) with an attenuated total reflection unit (GladiATR, PIKE Technologies, USA), with the same procedure as the literature[5].

Small-angle X-ray scattering (SAXS)

SAXS was performed using a small-angle instrument installed at beamline BL-6A at the Photon Factory, High Energy Accelerator Research Organization (Tsukuba, Japan)[6], with the same procedure as the literature[5]. The hot-pressed polymer film with a thickness of ~0.3 mm was directly placed on a rotary sample changer. Each sample was exposed to X-rays with a wavelength λ = 1.500 Å for 10 s. The scattered X-rays were collected by a two-dimensional detector (PILATUS3-1M, Dectris, Switzerland). The sample-to-detector distance was ~2.6 m. The scattering images were corrected for incident beam flux, exposure time, absorption, and background scattering. The images were circularly averaged to obtain a one-dimensional intensity profile $I(q)$ as a function of the magnitude of the scattering vector $q = 4\pi\sin\theta/\lambda$ (2θ: the scattering angle). Silver behenate was used as a calibrant[7].

Dynamic mechanical analysis (DMA)

DMA was performed on DMS6100 (Seiko, Japan) in tensile mode. The basic operation method is the same as the literature[5]. A test piece with dimensions of 10 mm × 25 mm and a thickness of ~0.5 mm was cut out from the hot-pressed polymer film. The sample was first cooled to −50 °C and then heated to 250 °C at 3 °C min^{-1} while applying sinusoidal tensile strain with a frequency f of 0.5, 1, 2, 5, and 10 Hz. The storage modulus E', the loss modulus E'', and the loss tangent ($\tan\delta = E''/E'$) were obtained. Master curves of E' were prepared according to the time-temperature superposition principle.

Differential scanning calorimetry (DSC)

DSC was performed on a DSC6220 (Seiko, Japan) or a DSC 214 polyma (NETZSCH, Germany). The basic operation method is the same as the literature[5]. The sample (~10 mg) was sealed in an aluminum pan. First, the sample was rapidly cooled from room temperature to -110 °C and heated to 110 °C at a heating rate of 10 °C min^{-1}. Then, the sample was cooled to −140 °C and heated to 260 °C at a rate of 10 °C min^{-1}. The second heating trace was used for analysis.

Tensile tests

Tensile tests were performed on an AGS-X (Shimadzu, Japan) equipped with a 100 N load cell, with the same procedure as the literature[5]. The dumbbell-shaped sample (ISO 37-4 shrunk by 2/3, the initial length of the parallel section was 8 mm) with a thickness of ~0.3 mm was cut from the hot-pressed polymer film. All test pieces were dried in vacuo at room temperature for at least 24 h prior to the tests to eliminate possible influences of water absorption. The test piece was stretched at a constant crosshead speed of 50 mm min^{-1}, which corresponded to a nominal strain rate of 0.1 s^{-1}. At least three test pieces were tested, and their mean and standard deviation were calculated. In the cyclic tensile test, the test piece was loaded to 150% strain at a crosshead speed of 50 mm min^{-1} and then unloaded to its initial length at the same speed. The loading–unloading cycle was repeated 4 more times with varying waiting times before each cycle (1 min, 30 min, 1 h, and 3 h). The cyclic tensile test was performed on one test piece for each sample. All the tests were conducted at room temperature. All the strain and the stress reported are the nominal strain and engineering stress, respectively.

Stress relaxation test

Stress relaxation test was performed on an AGS-X (Shimadzu, Japan) equipped with a 100 N load cell. The test pieces were the same as for the tensile test. The test piece was loaded to 1.0 MPa stress or 100% strain at a crosshead speed of 50 mm min^{-1} and then kept at the corresponding strain for 30 minutes. The stress-relaxation test was performed on one test piece for each sample. All the stress reported is the engineering stress.

Density functional theory (DFT) calculation

Density functional theory (DFT) calculation was carried out with the Gaussian 16W program[8]. B3LYP/6-311G(d,p) level was used for all the DFT calculations. First, the structure of the small model compounds was optimized. Then, the possible H-bonds dimers between the optimized structure were created and optimized. The optimized dimer structure and the corresponding binding energy were corrected by basis set superposition error (BSSE) method. The corrected data was used as the binding energy value ΔE due to H-bonding.

General procedure to determine comonomer conversions

Figure S1 shows ^{1}H NMR spectrum of reaction mixture as an example. Peaks a, b, c, and d correspond to olefin signal of norbornene monomer (5.85-6.25 ppm), olefin signal of polymerized norbornene backbone (5.10-5.65 ppm), the signal of hydrocarbon adjacent to ester group with Dodec (M_2) or polymerized Dodec (P_2) (3.85-4.15 ppm), the signal of hydrocarbon adjacent to protected hydroxyl group with (2,2)DiOTBS (M_1) (3.55-3.80 ppm), respectively. The relationship between each peak intensity and the number of monomers is described by the following equations:

$$\frac{a}{2} = M_1 + M_2 \tag{S1}$$

$$\frac{b}{2} = P_1 + P_2 \tag{S2}$$

$$\frac{c}{2} = M_2 + P_2 \tag{S3}$$

$$d = M_1 \tag{S4}$$

Therefore, those ratios between M1, M2, P1, and P2 at the reaction time are calculated by the following equations:

$$M_1 = d \tag{S5}$$

$$M_2 = \frac{a}{2} - d \tag{S6}$$

$$P_1 = \frac{a}{2} + \frac{b}{2} - \frac{c}{2} - d \tag{S7}$$

$$P_2 = -\frac{a}{2} + \frac{c}{2} + d \tag{S8}$$

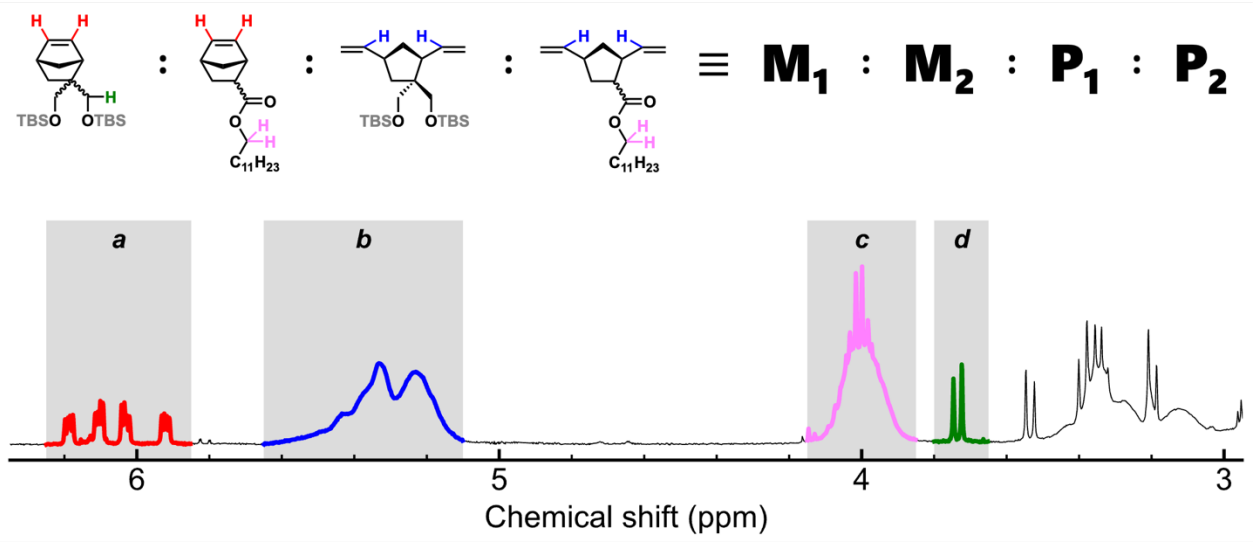

Figure S1. Peaks in ^{1}H NMR spectrum of the reaction mixture used to determine monomer conversion. The spectrum shown was taken during the synthesis of (2,2)DiOTBS-120 at 90 min.

2. Additional figures

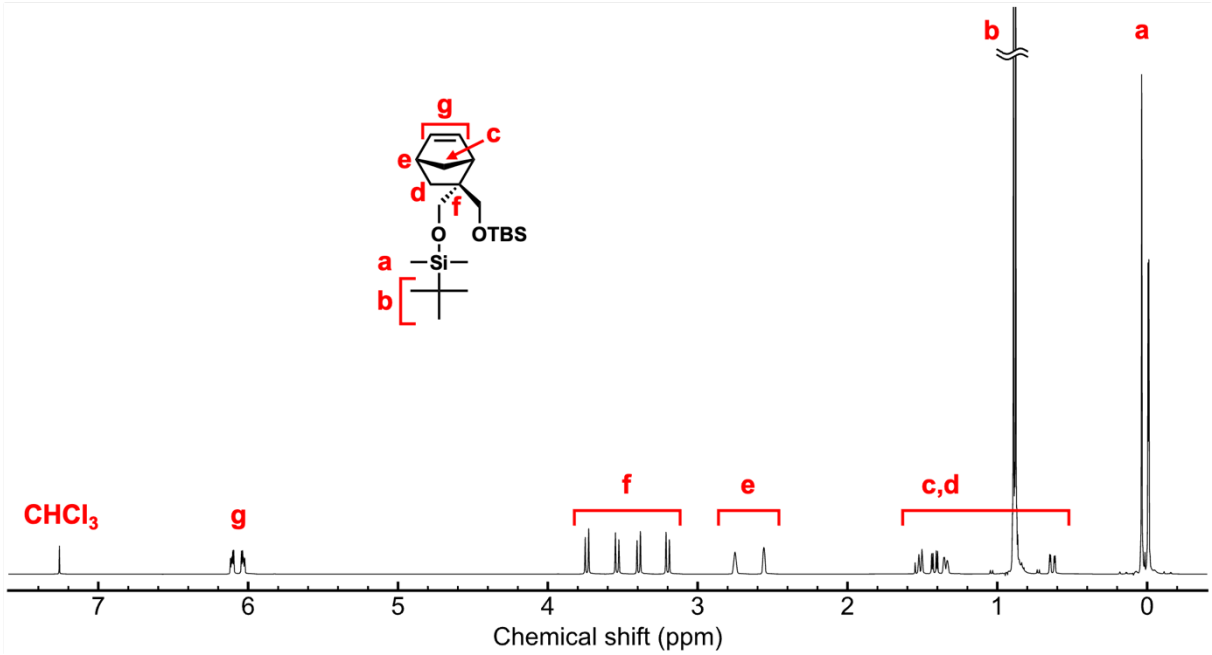

Figure S2. ^{1}H NMR spectrum of (2,2)DiOTBS ($CDCl_3$, 400 MHz, internal standard: 7.26 ppm from $CHCl_3$).

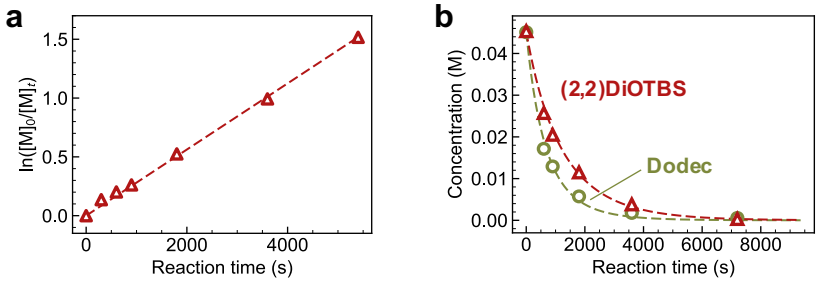

Figure S3. (a) First-order kinetic plot of the monomer conversion against the reaction time for homopolymerization of (2,2)DiOTBS. Dashed line indicates the results of linear fitting, resulting in propagation rate constant $k_{homo,\ (2,2)Diol}$ = 2.49 M^{-1} s^{-1}. Homopolymerization analysis of (2,2)DiOTBS was done in the same manner as in the literature[5]. (b) Concentration of (2,2)DiOTBS and Dodec as a function of reaction time in one-pot copolymerization. Dashed curves show the model with optimized rate constants, resulting in propagation rate constant $k_{Dodec,\ (2,2)Diol}$ = 8.92 M^{-1} s^{-1} and $k_{Dodec,\ (2,2)Diol}$ = 2.85 M^{-1} s^{-1}. Copolymerization analysis of (2,2)DiOTBS and Dodec was done in the same manner as in the literature[5].

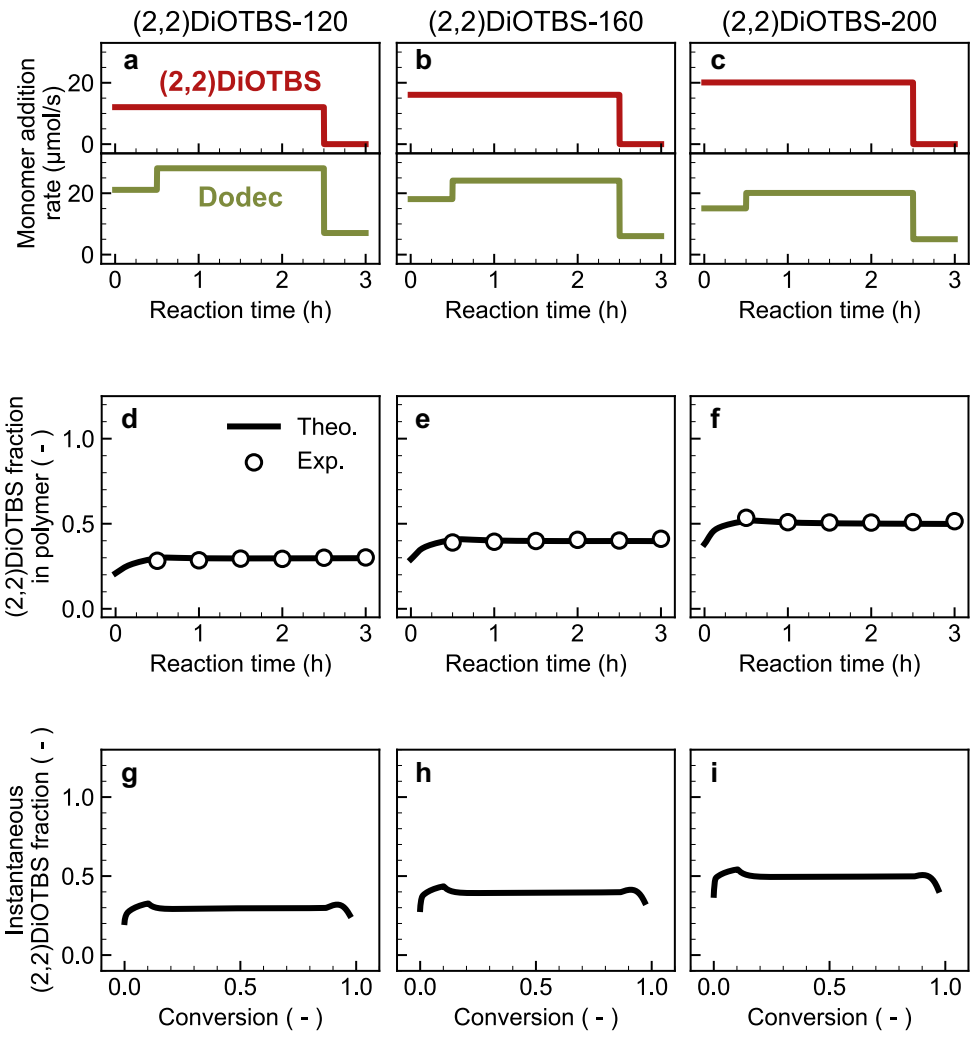

Figure S4. (a-c) Comonomer addition schedules shown as the addition rate of each comonomer as a function of the reaction time for the synthesis of (a) (2,2)DiOTBS-120, (b) (2,2)DiOTBS-160, and (c) (2,2)DiOTBS-200. (d-f) (2,2)DiOTBS fraction in the polymer chains versus the reaction time in (d) (2,2)DiOTBS-120, (f) (2,2)DiOTBS-160, and (g) (2,2)DiOTBS-200. The experimental data are plotted with open circles. Solid curves represent the simulation results based on the framework for controlling the monomer sequence. (g-i) Instantaneous (2,2)DiOTBS fraction (i.e., comonomer distribution along the polymer chain) in (g) (2,2)Diol-120, (h) (2,2)Diol-160, (i) (2,2)Diol-200.

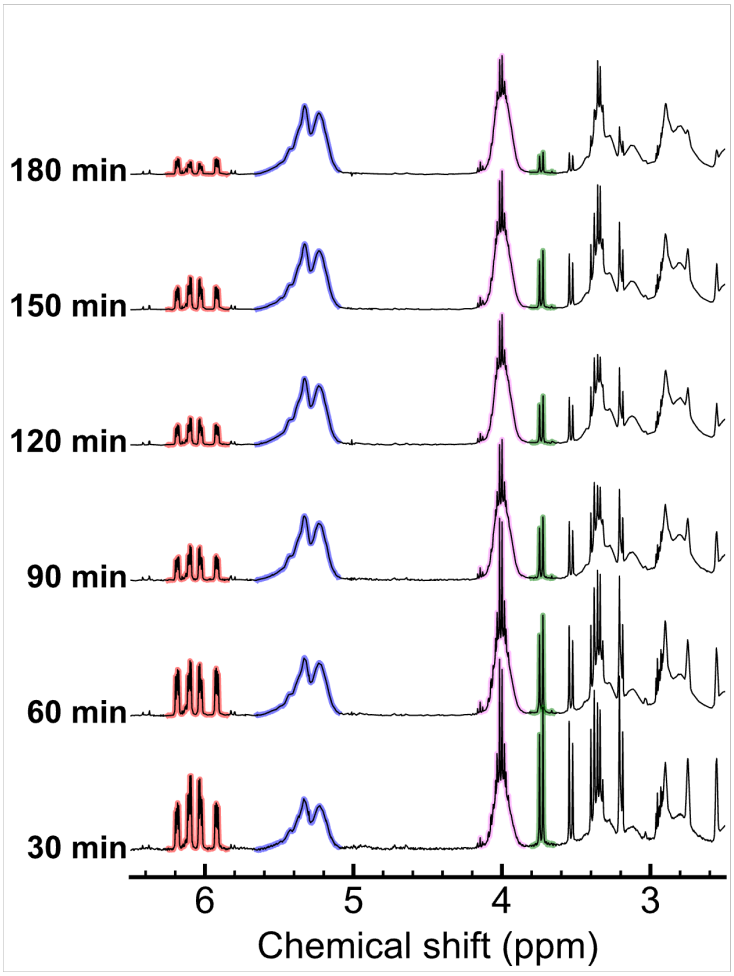

Figure S5. ^{1}H NMR spectrum of reaction mixture in (2,2)DiOTBS-120 ($CDCl_3$, 400 MHz, internal standard: 7.26 ppm from $CHCl_3$). The peaks used to estimate comonomer conversions are indicated in color.

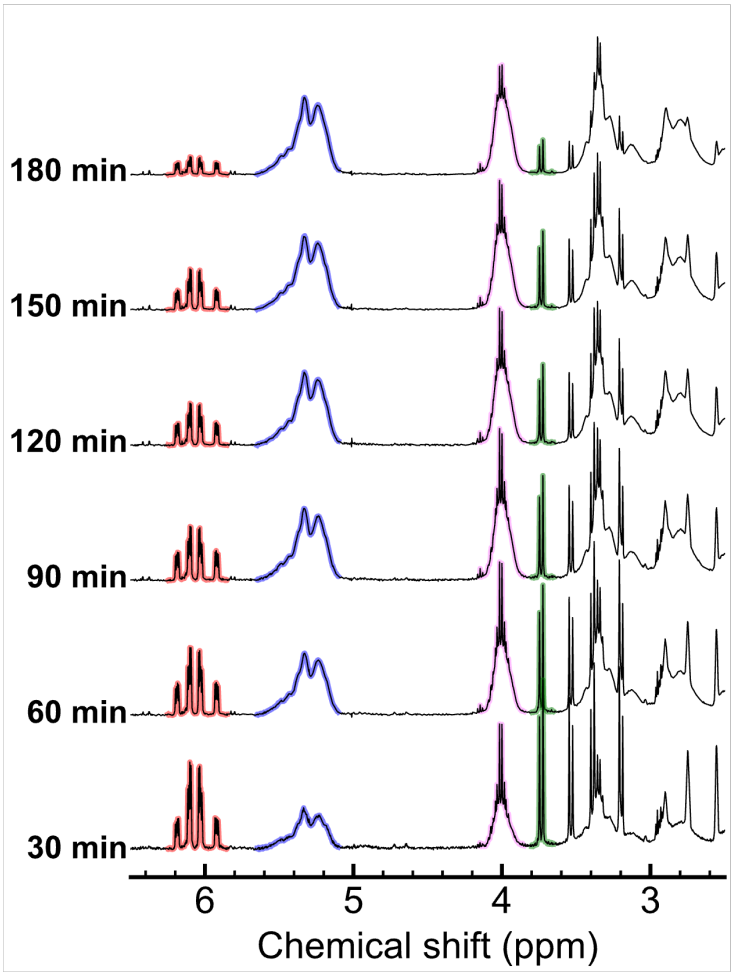

Figure S6. ^{1}H NMR spectrum of reaction mixture in (2,2)DiOTBS-160 ($CDCl_3$, 400 MHz, internal standard: 7.26 ppm from $CHCl_3$). The peaks used to estimate comonomer conversions are indicated in color.

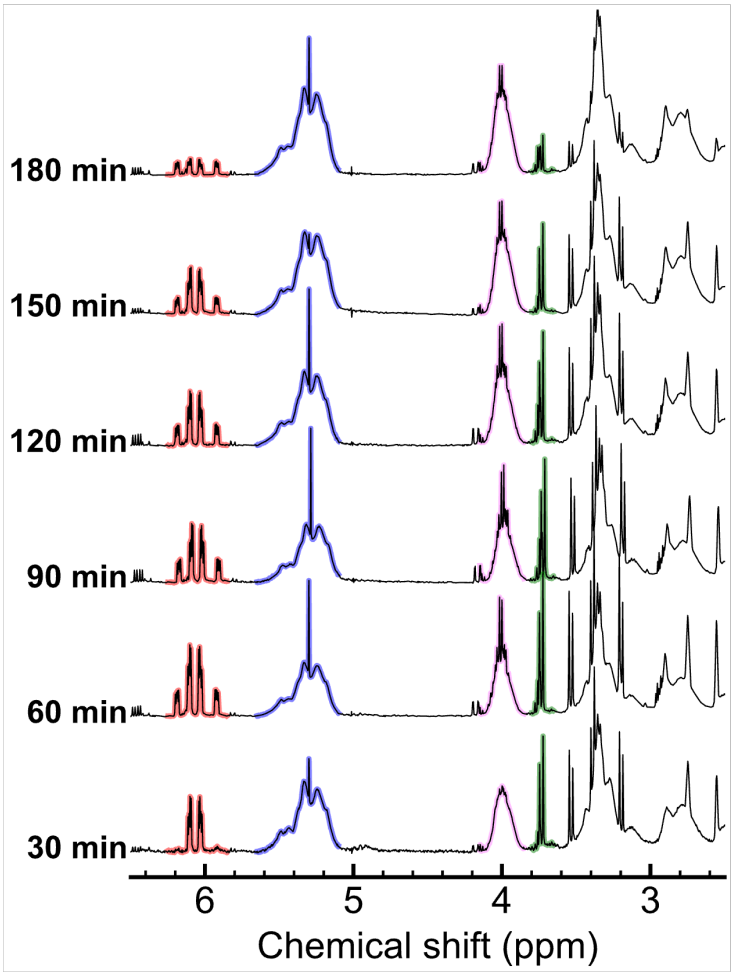

Figure S7. ^{1}H NMR spectrum of reaction mixture in (2,2)DiOTBS-200 ($CDCl_3$, 400 MHz, internal standard: 7.26 ppm from $CHCl_3$). The peaks used to estimate comonomer conversions are indicated in color.

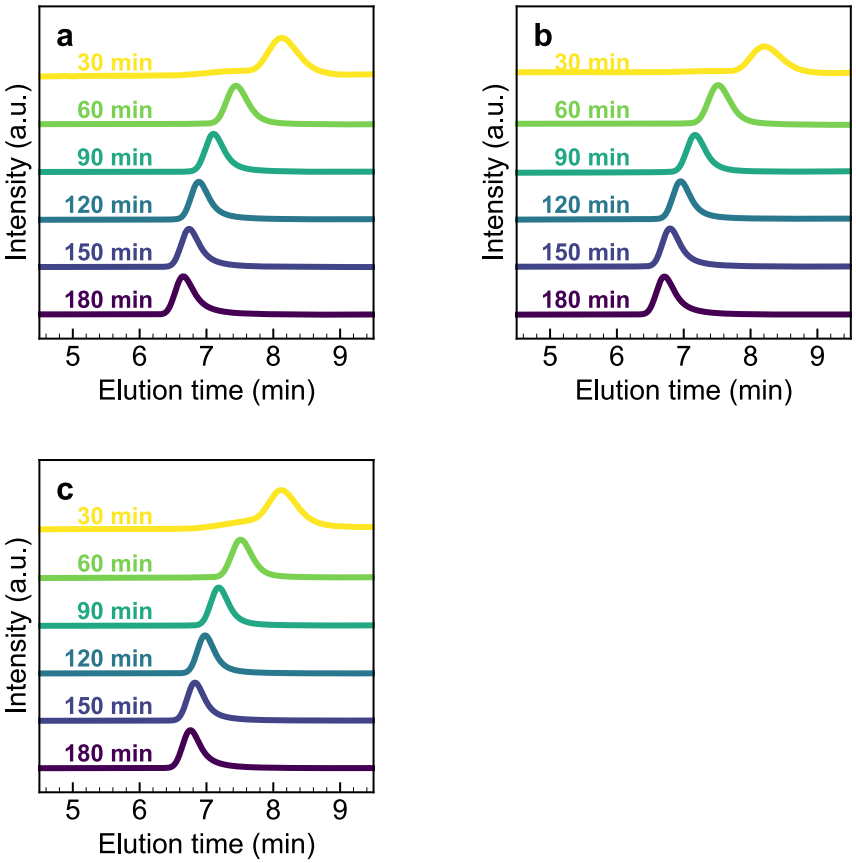

Figure S8. SEC profiles of the reaction mixture for (2,2)DiOTBS-*x*. (a) *x* = 120, (b) *x* = 160, and (c) *x* = 200.

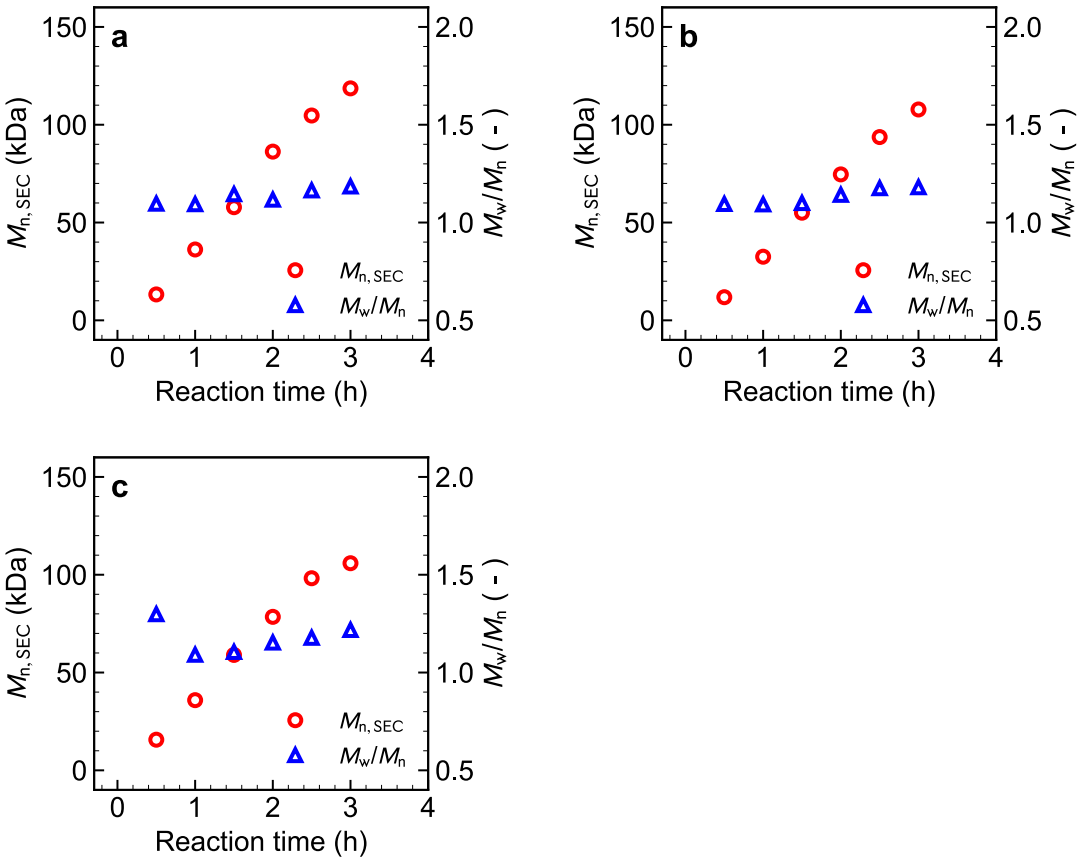

Figure S9. $M_{n,SEC}$ and M_w/M_n, of (2,2)DiOTBS-*x* determined by SEC, plotted as a function of the reaction times. (a) $x = 120$, (b) $x = 160$, and (c) $x = 200$.

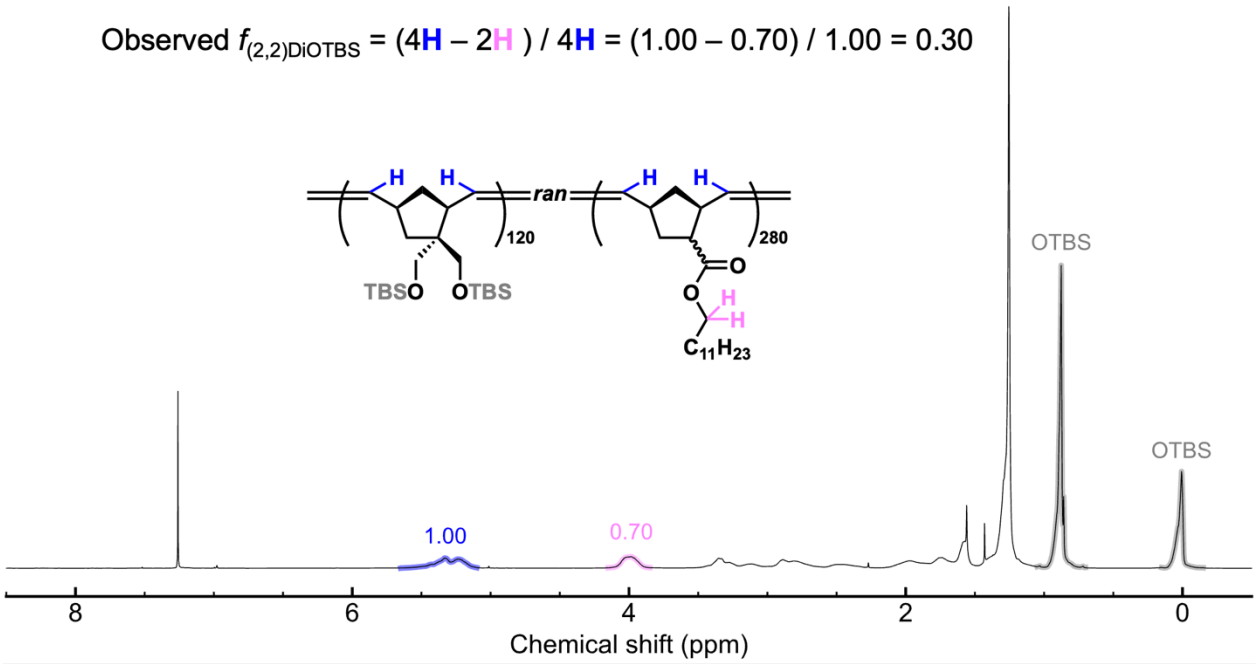

Figure S10. ^{1}H NMR spectrum of (2,2)DiOTBS-120 ($CDCl_3$, 400 MHz, internal standard: 7.26 ppm from $CHCl_3$).

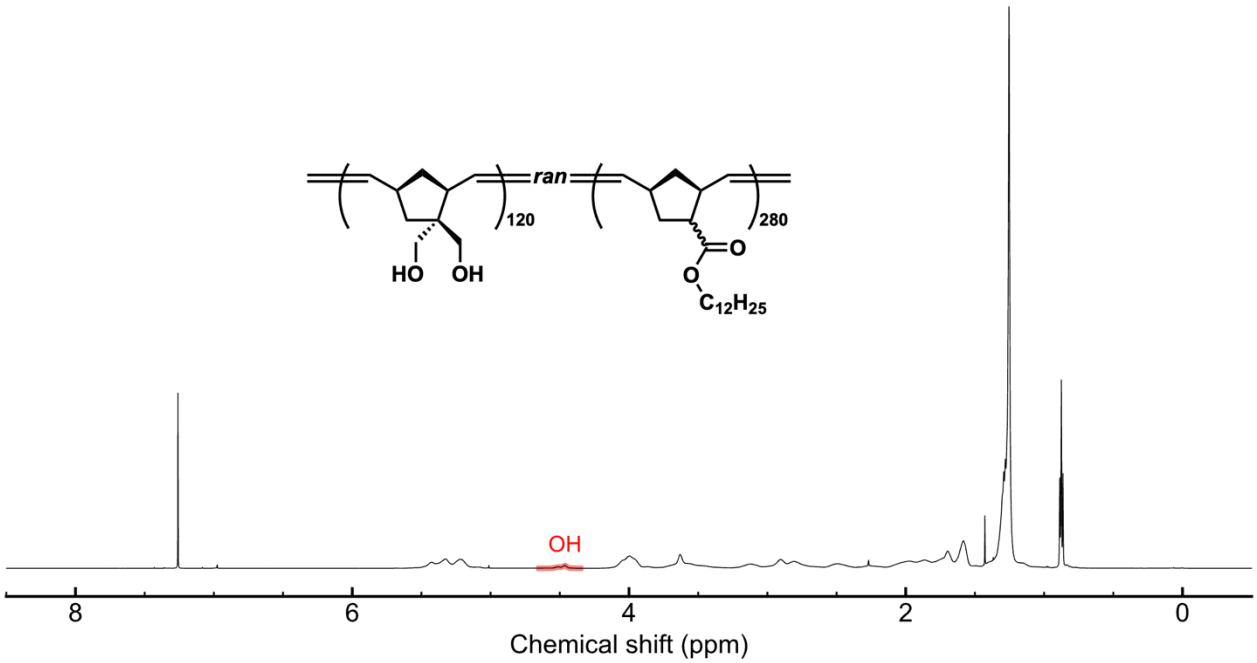

Figure S11. ^{1}H NMR spectrum of (2,2)Diol-120 ($CDCl_3$, 600 MHz, internal standard: 7.26 ppm from $CHCl_3$).

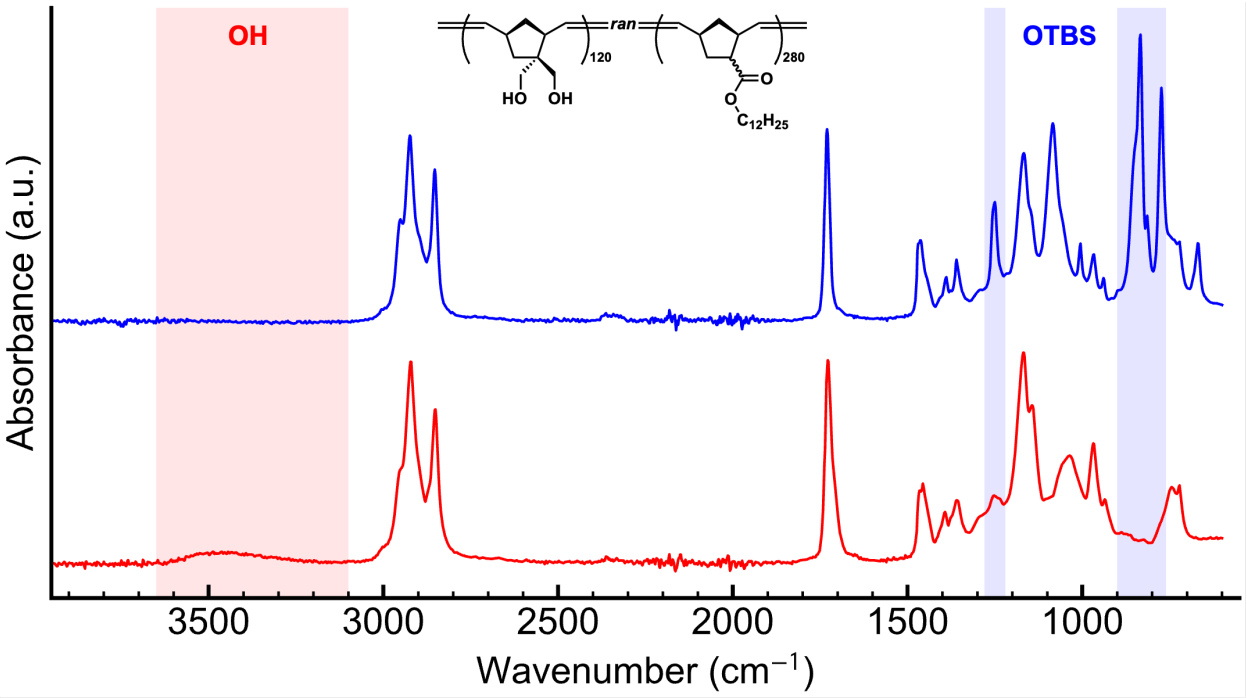

Figure S12. IR spectra of (2,2)DiOTBS-120 (blue line) and (2,2)Diol-120 (red line).

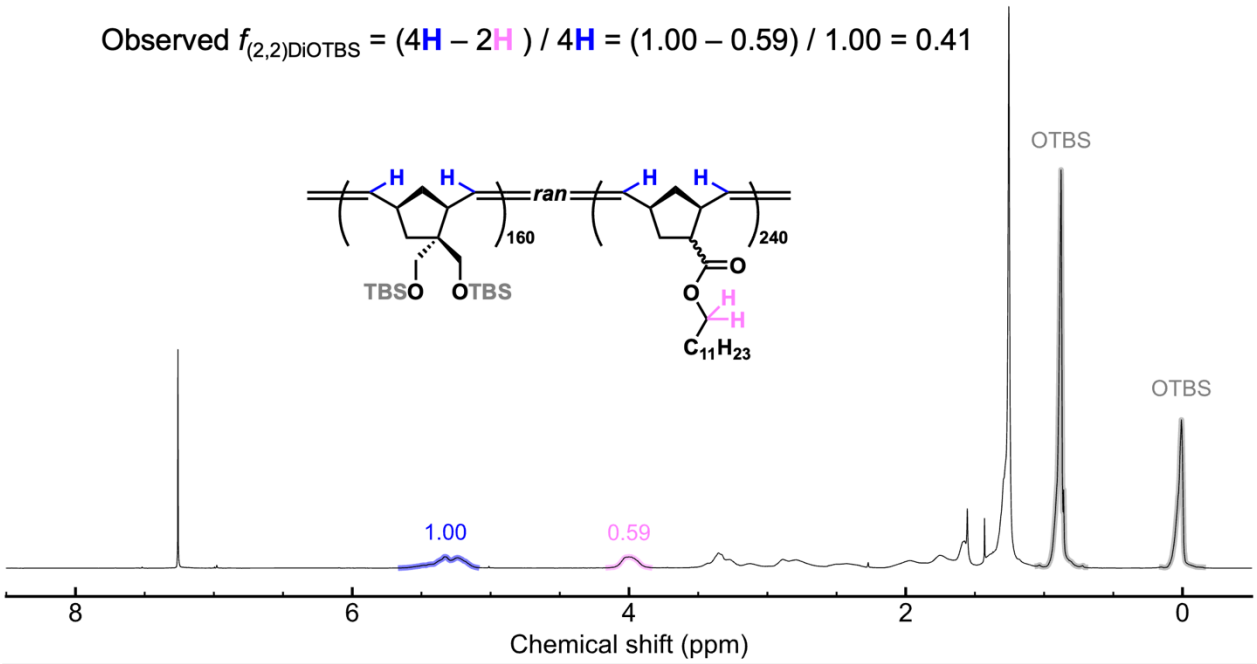

Figure S13. ^{1}H NMR spectrum of (2,2)DiOTBS-160 ($CDCl_3$, 400 MHz, internal standard: 7.26 ppm from $CHCl_3$).

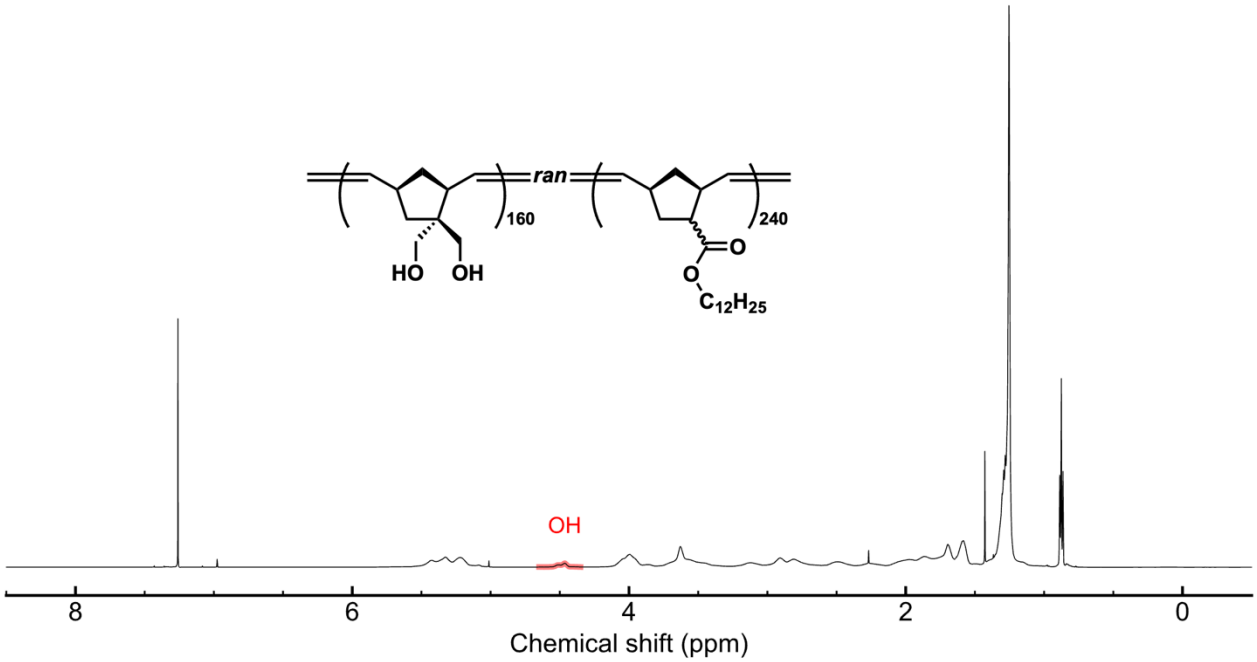

Figure S14. ^{1}H NMR spectrum of (2,2)Diol-160 ($CDCl_3$, 600 MHz, internal standard: 7.26 ppm from $CHCl_3$).

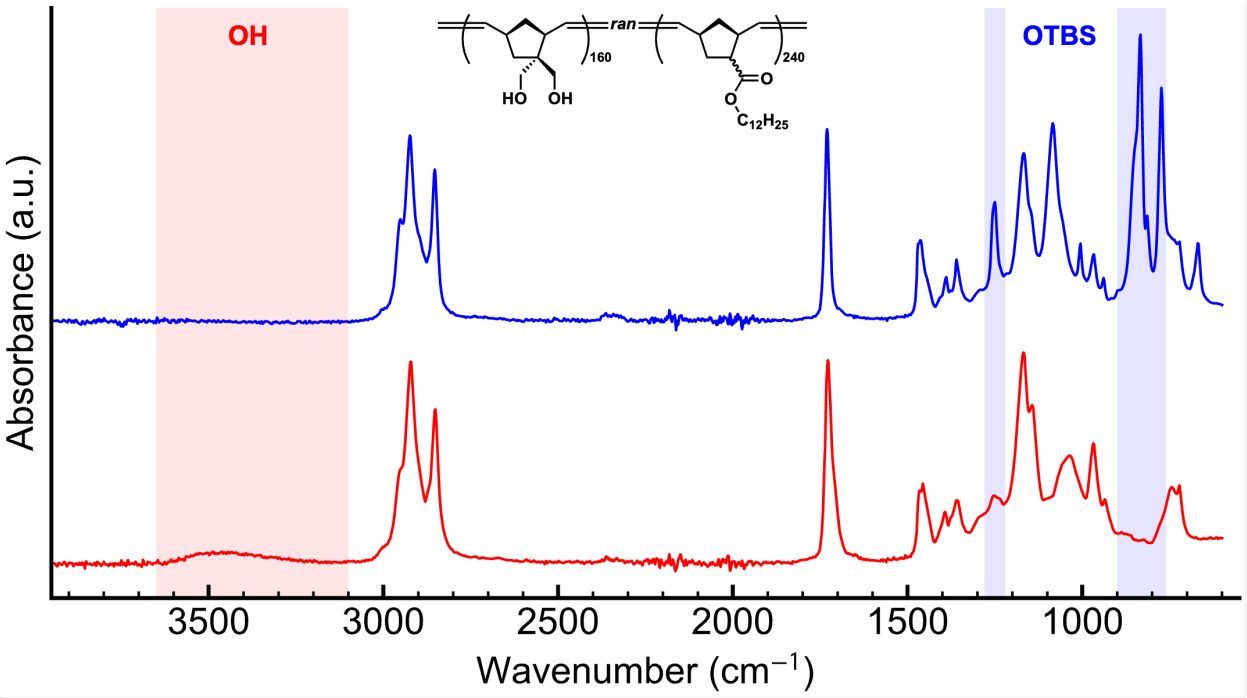

Figure S15. IR spectra of (2,2)DiOTBS-160 (blue line) and (2,2)Diol-160 (red line).

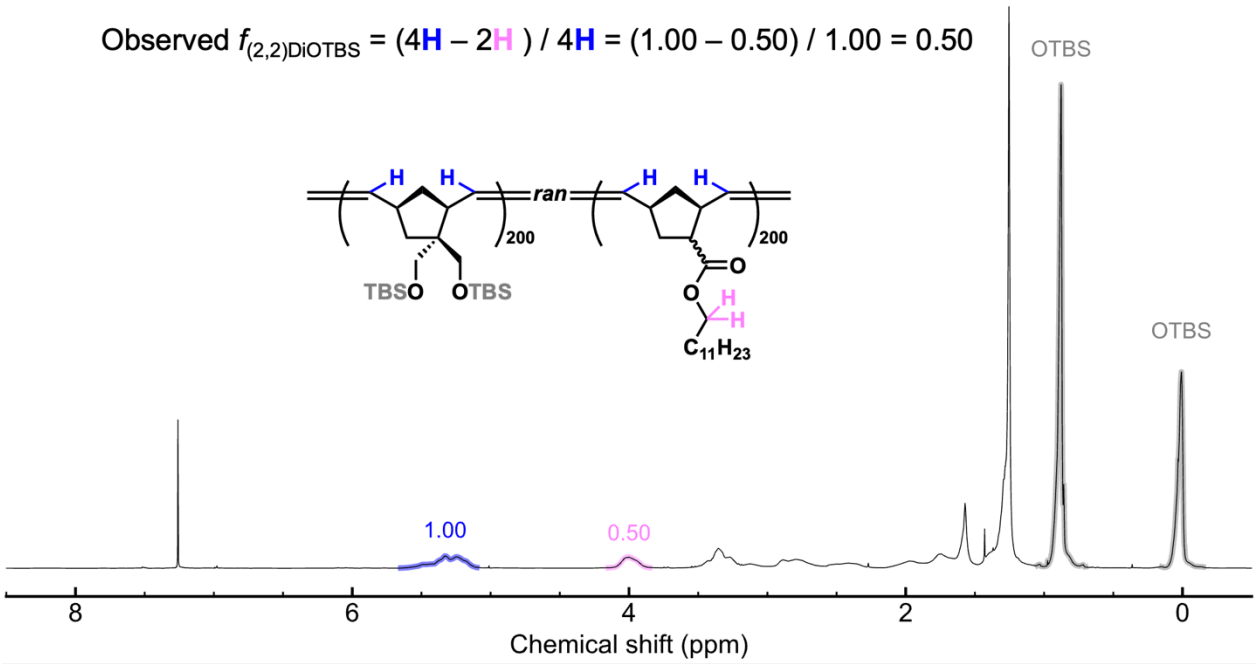

Figure S16. ^{1}H NMR spectrum of (2,2)DiOTBS-200 ($CDCl_3$, 400 MHz, internal standard: 7.26 ppm from $CHCl_3$).

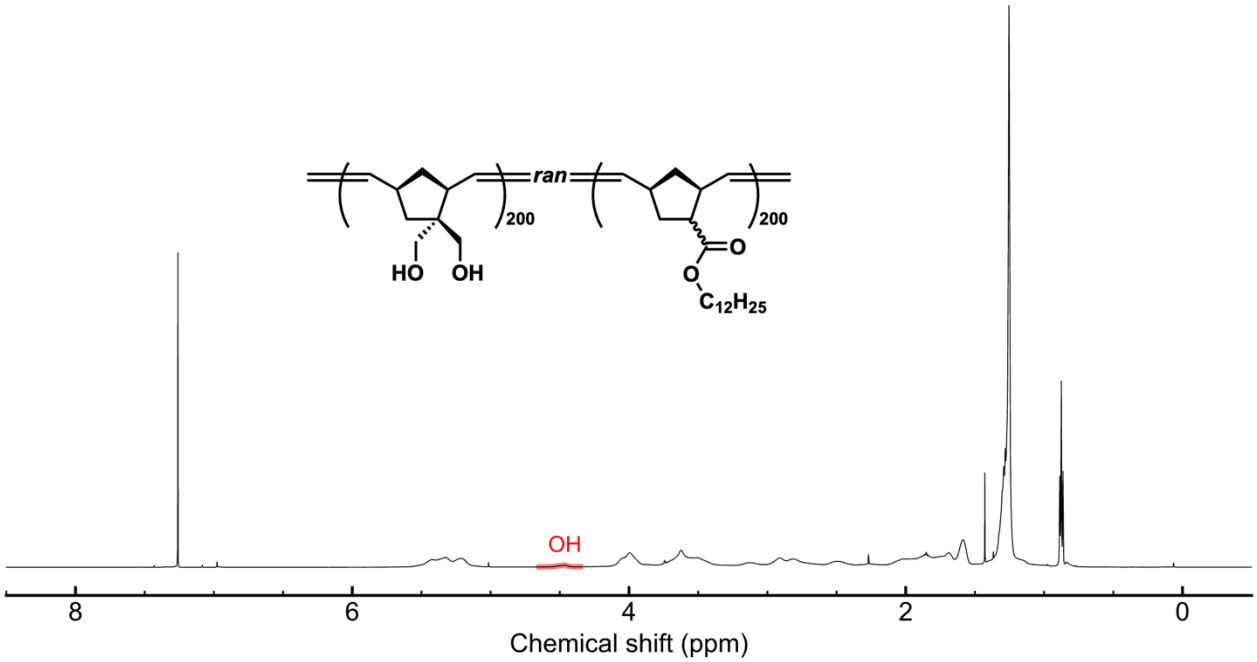

Figure S17. ^{1}H NMR spectrum of (2,2)Diol-200 ($CDCl_3$, 600 MHz, internal standard: 7.26 ppm from $CHCl_3$).

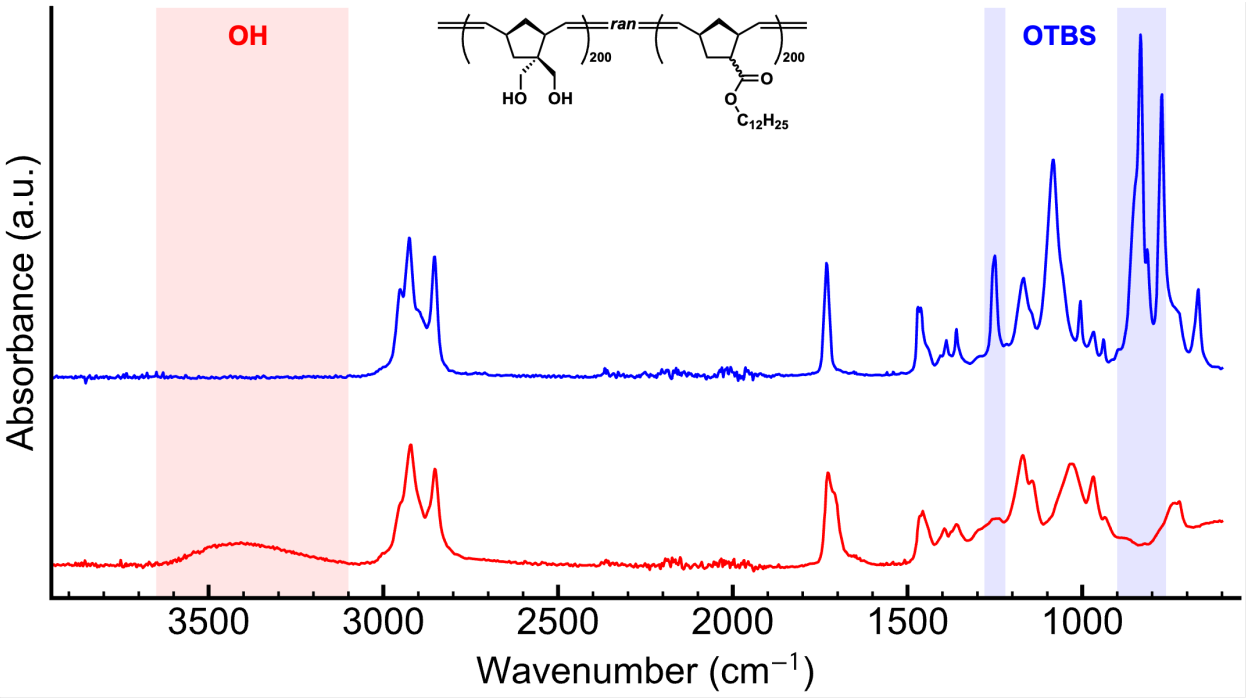

Figure S18. IR spectra of (2,2)DiOTBS-200 (blue line) and (2,2)Diol-200 (red line).

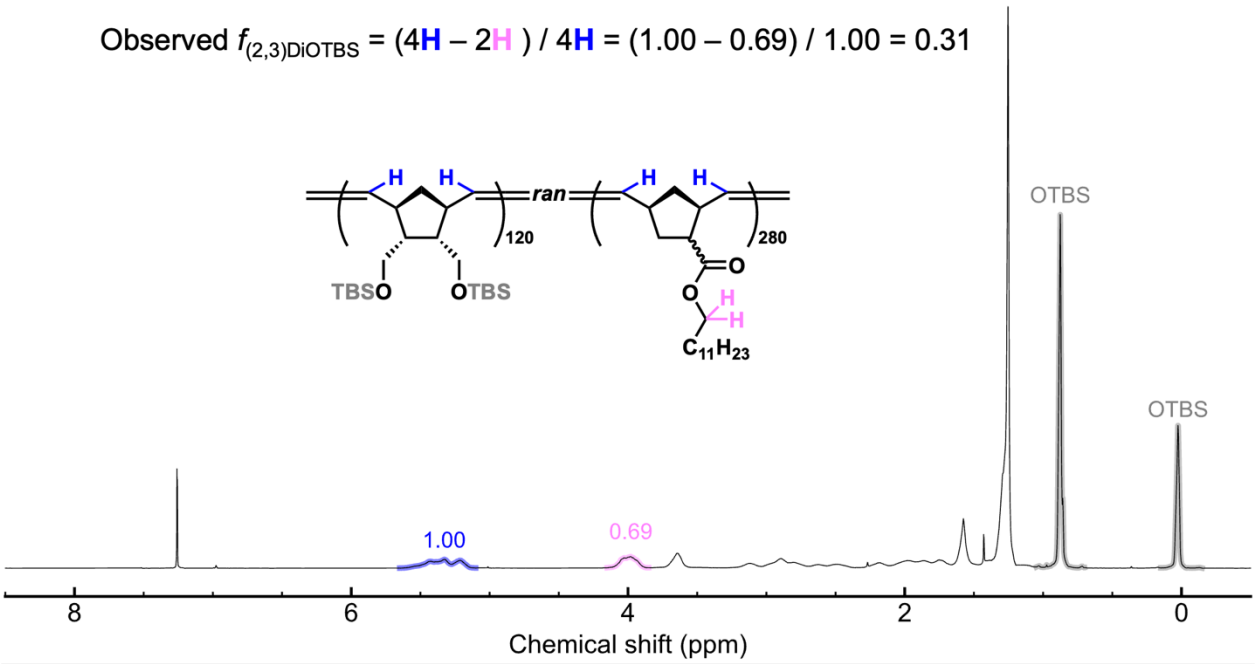

Figure S19. ^{1}H NMR spectrum of (2,3)DiOTBS-120 ($CDCl_3$, 400 MHz, internal standard: 7.26 ppm from $CHCl_3$). The data is identical to the one reported in our previous study[4] and is presented here just for the sake of completeness.

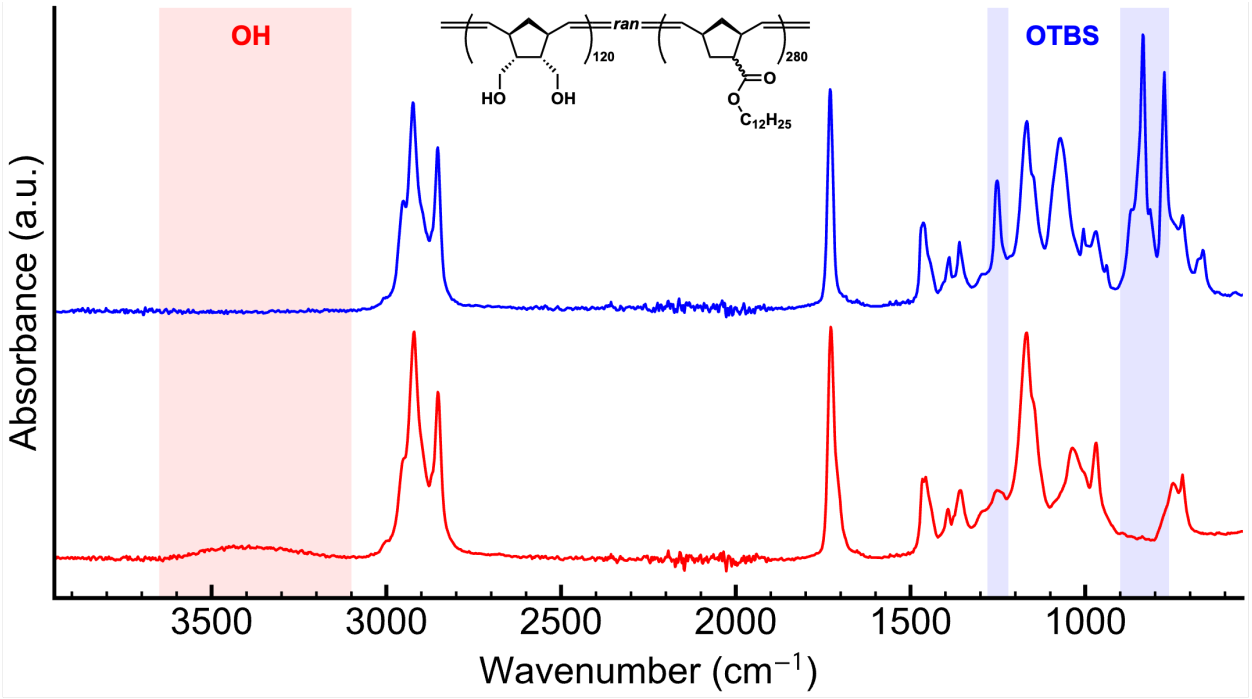

Figure S20. IR spectra of (2,3)DiOTBS-120 (blue line) and (2,3)Diol-120 (red line).

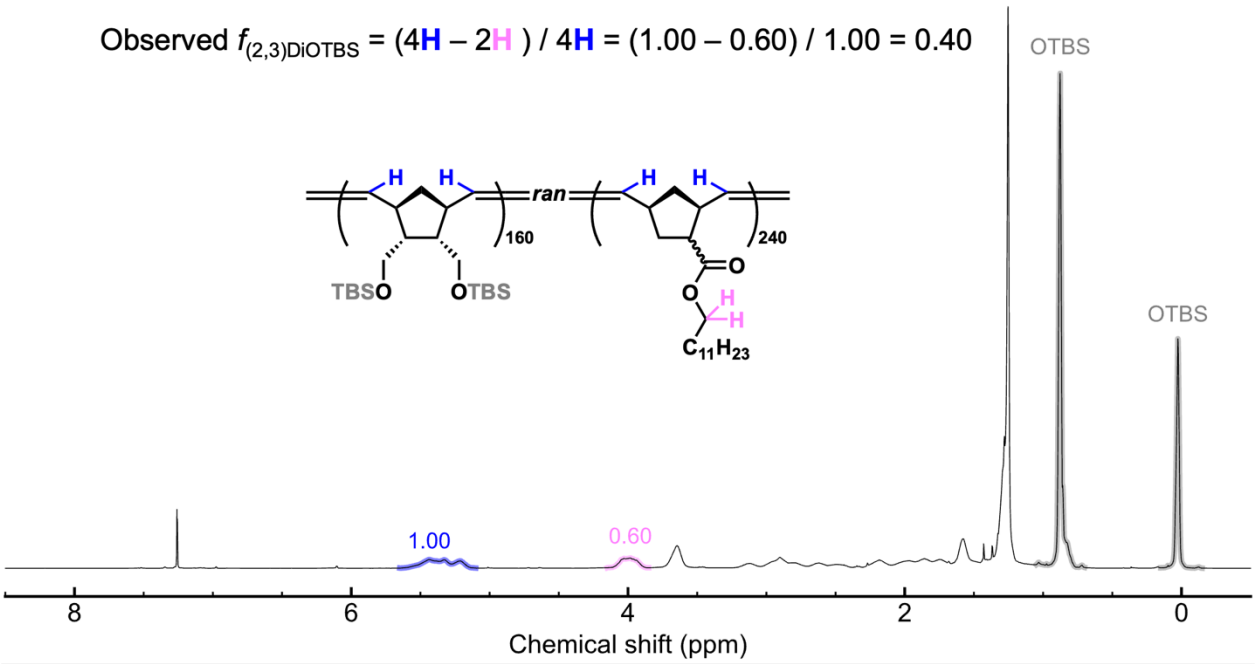

Figure S21. ^{1}H NMR spectrum of (2,3)DiOTBS-160 ($CDCl_3$, 400 MHz, internal standard: 7.26 ppm from $CHCl_3$). The data is identical to the one reported in our previous study[4] and is presented here just for the sake of completeness.

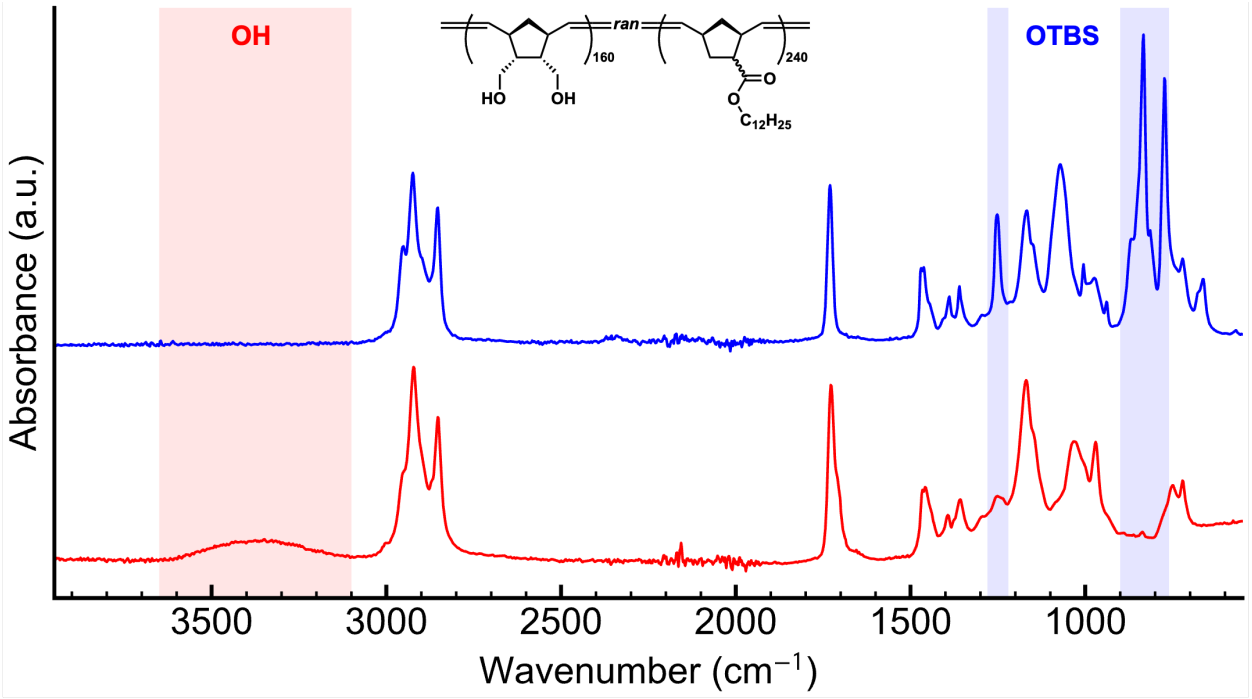

Figure S22. IR spectra of (2,3)DiOTBS-160 (blue line) and (2,3)Diol-160 (red line).

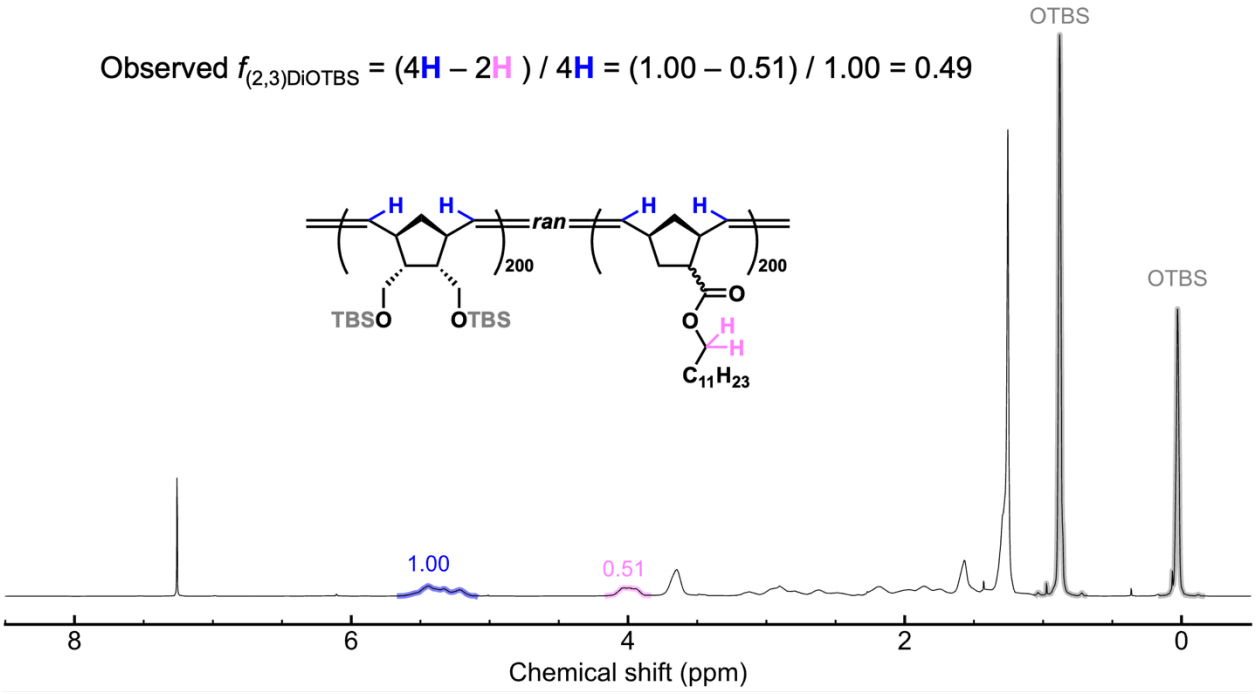

Figure S23. ^{1}H NMR spectrum of (2,3)DiOTBS-200 ($CDCl_3$, 400 MHz, internal standard: 7.26 ppm from $CHCl_3$). The data is identical to the one reported in our previous study[4] and is presented here just for the sake of completeness.

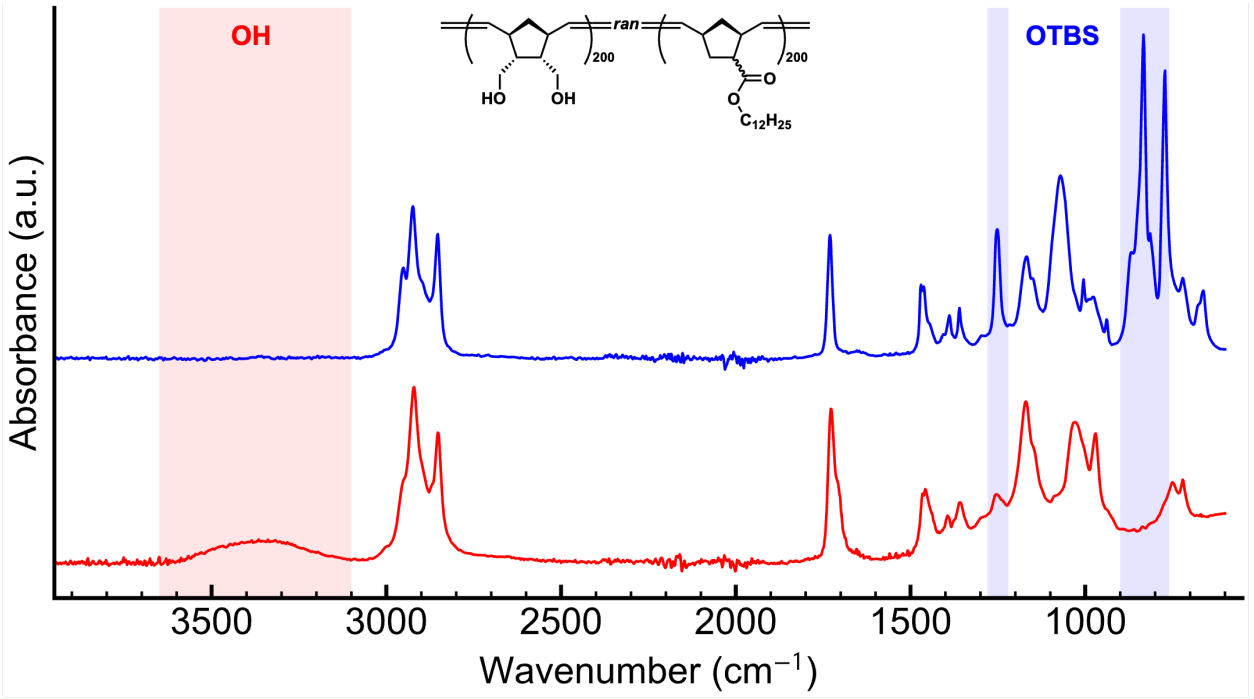

Figure S24. IR spectra of (2,3)DiOTBS-200 (blue line) and (2,3)Diol-200 (red line).

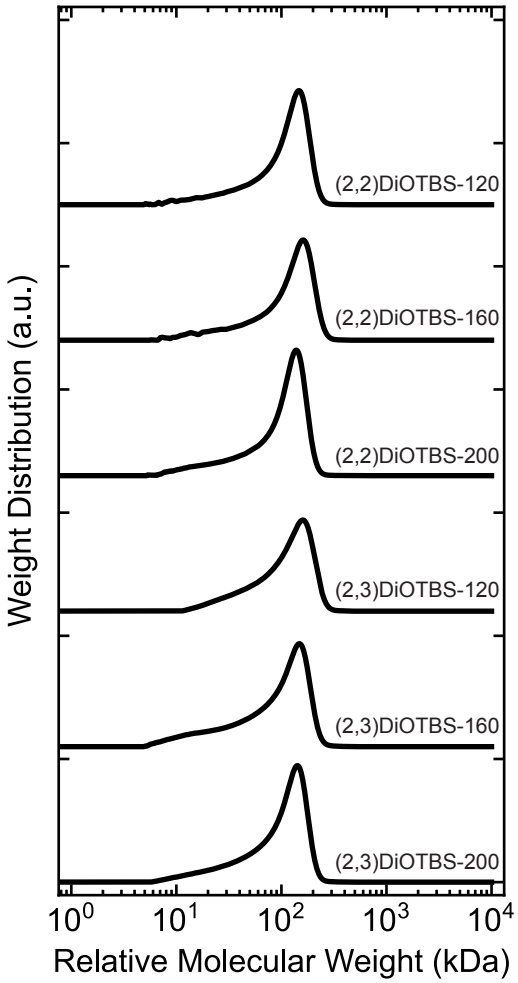

Figure S25. Weight distribution of relative molecular weight of isolated (2,2)DiOTBS-*x* and (2,3)DiOTBS-*x* (*x* = 120, 160, and 200) derived from SEC profiles. The profiles of (2,3)DiOTBS-*x* were plotted by using the data reported in our previous study[4].

Table S1. Characterization of the polymers.

Sample	Before deprotection					After deprotection
	DiOTBS/Dodec		Theo.	Obs.	Obs.	Theo.
	Feed	Obs.[a]	M_n (kDa) [b]	$M_{n,SEC}$ (kDa) [c]	M_w/M_n [c]	M_n (kDa) [b]
(2,2)Diol-120	30/70	30/70	132	121	1.17	104
(2,2)Diol-160	40/60	41/59	135	130	1.19	98
(2,2)Diol-200	50/50	50/50	138	109	1.21	92
(2,3)Diol-120[d]	30/70	31/69	132	119	1.26	104
(2,3)Diol-160[d]	40/60	40/60	135	102	1.34	98
(2,3)Diol-200[d]	50/50	49/51	138	106	1.25	92

a. Observed DiOTBS/Dodec ratio in the product was determined by ^{1}H NMR spectroscopy.

b. Theoretical molecular weight was calculated from the feed ratio of monomer to catalyst.

c. Observed molecular weight was determined by SEC with polystyrene standards.

d. The data was reproduced from our previous study[5].

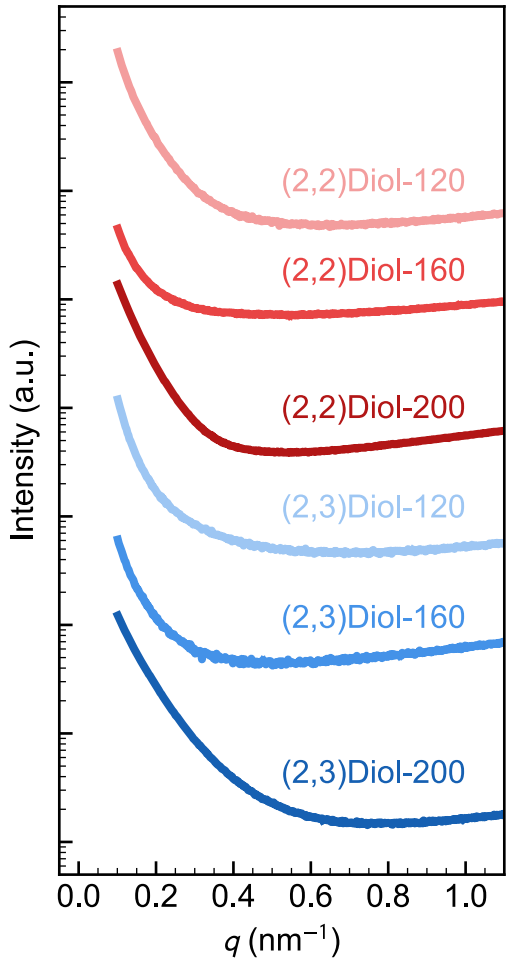

Figure S26. SAXS profiles of (2,2)Diol-*x* and (2,3)Diol-*x*. The profiles have been shifted vertically for legibility.

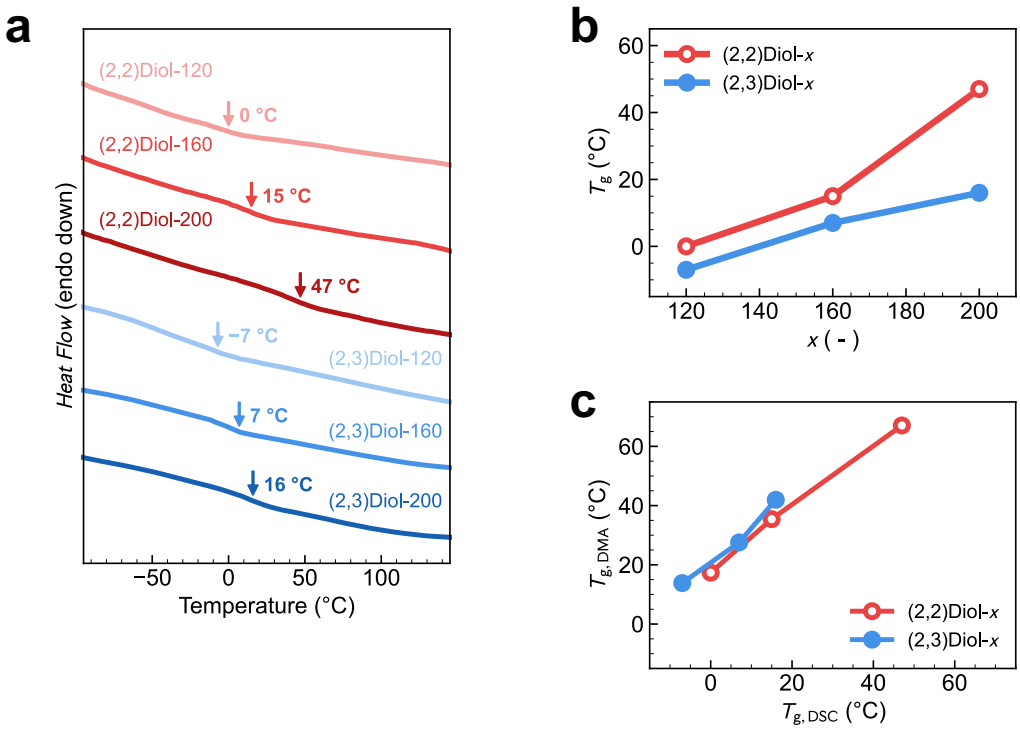

Figure S27. (a) DSC thermograms of (2,2)Diol-*x* and (2,3)Diol-*x*. (b) T_g of the copolymers plotted against *x*. (c) The T_g measured by DSC plotted against the T_g measured by DMA.

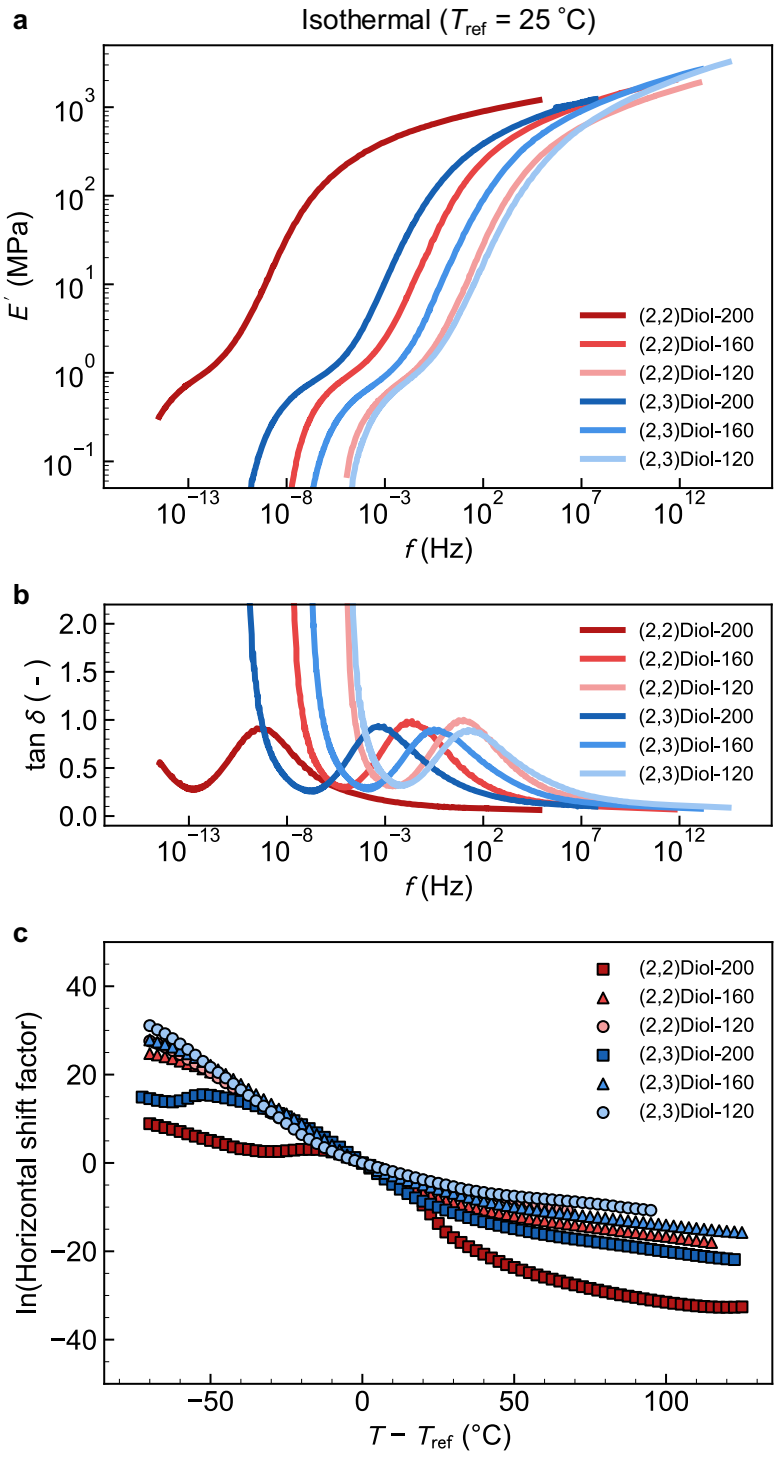

Figure S28. Isothermal master curves and associated shift factors of (2,2)Diol-*x* and (2,3)Diol-*x* constructed at T_{ref} = 25 °C. (a) Master curves of *E'*. (b) Master curves of tan δ. (c) Horizontal shift factors plotted against $T - T_{ref}$.

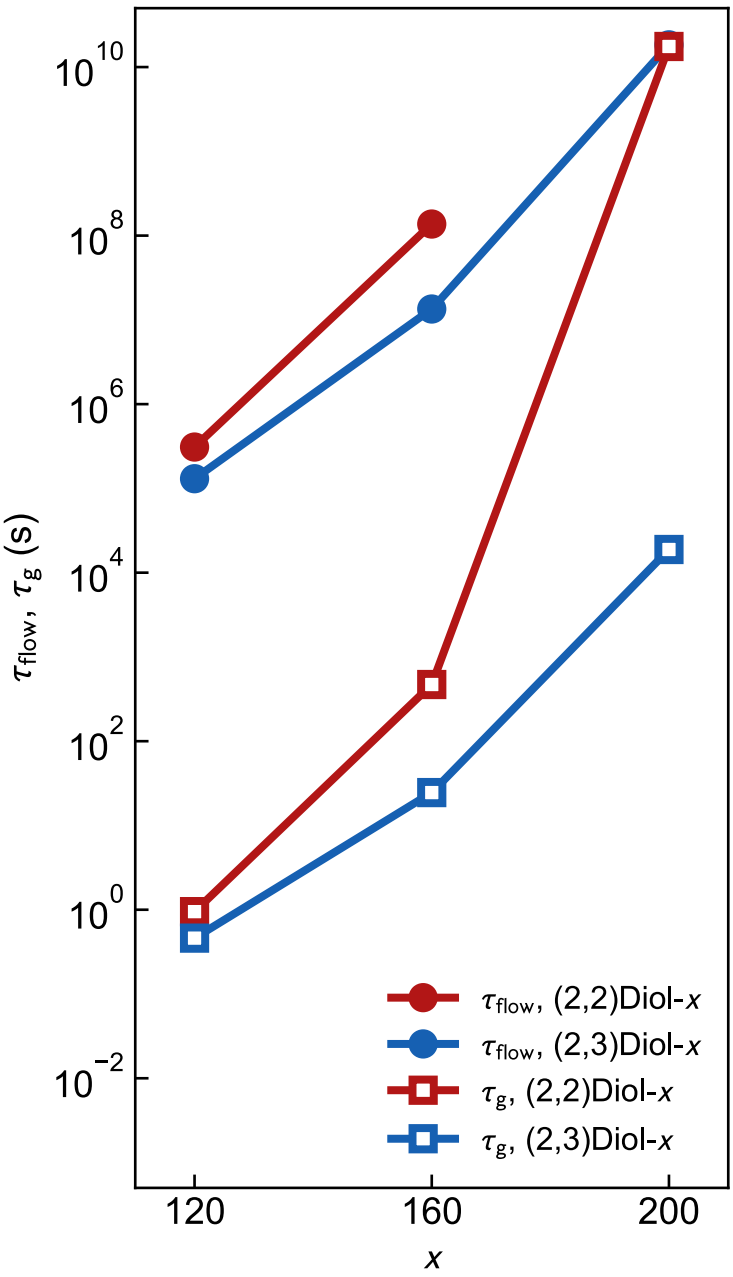

Figure S29. Relaxation time associated with the glass transition τ_g and relaxation time of terminal flow τ_{flow} for (2,2)Diol-x and (2,3)Diol-x at T_{ref} = 25 °C, plotted as a function of x. τ_g was defined as the inverse of frequency at tan δ peak in the isothermal master curve. τ_{flow} was defined as the inverse of frequency at the point where tan δ = 1. τ_{flow} of (2,2)-Diol-200 could not be evaluated because the tan δ master curve did not rise above unity in the temperature and frequency range investigated.

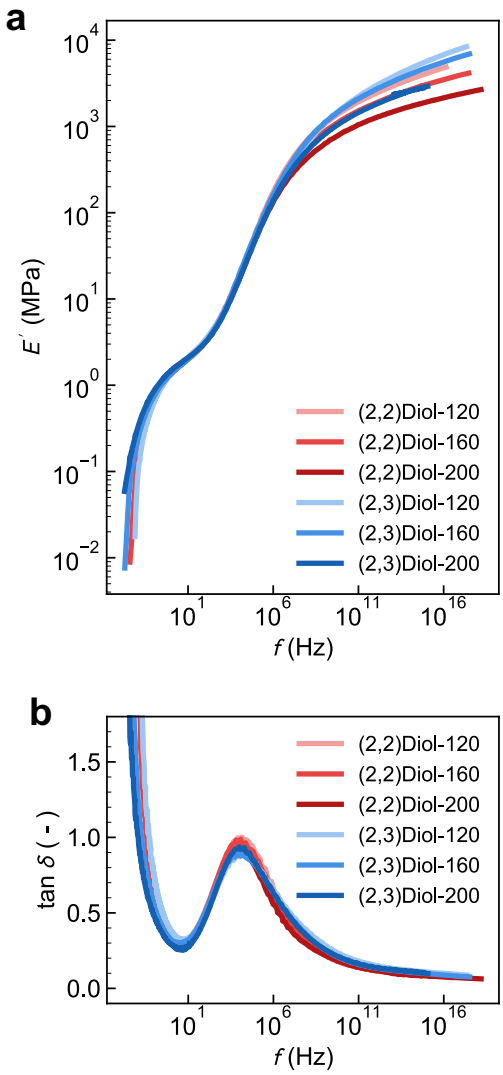

Figure S30. Isofrictional master curves of (2,2)Diol-*x* and (2,3)Diol-*x* constructed at $T_{ref} = T_g + 50$ K. (a) Master curves of *E'*. Vertical shifts have been applied to all curves except for (2,3)Diol-200, so that all other curves overlap well with that of (2,3)Diol-200 in the rubbery plateau region. (b) Master curves of tan δ.

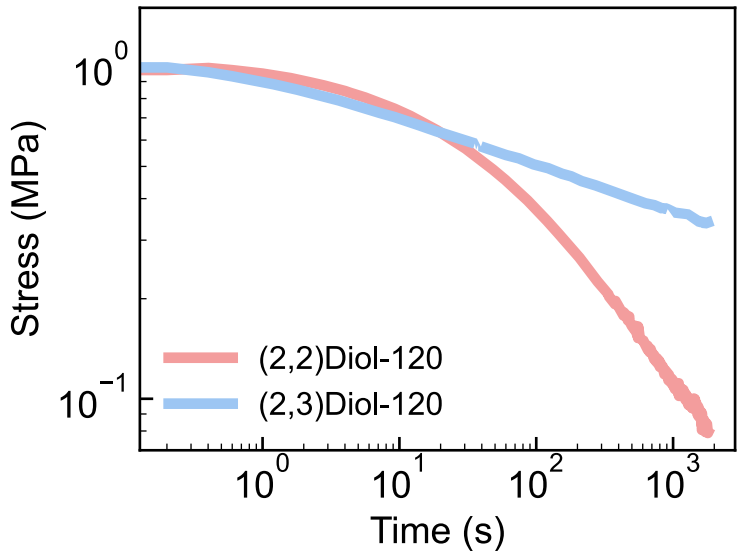

Figure S31. Stress relaxation curves of (2,2)Diol-120 and (2,3)Diol-120, obtained by applying the initial stress of ~ 1 MPa. The applied strain was 544% and 74% for (2,2)Diol-120 and (2,3)Diol-120, respectively.

3. Supplementary references

(1) Mayo, P.; Orlova, G.; Goddard, J. D.; Tam, W. Remote Substituent Effects on the Oxymercuration of 2-Substituted Norbornenes: An Experimental and Theoretical Study. *J. Org. Chem.* **2001**, *66* (15), 5182–5191. https://doi.org/10.1021/jo010330h.

(2) Kang, E.-H.; Yang, S.; Yu, S. Y.; Kim, J.; Choi, T.-L. Spontaneous Evolution of Nanostructures by Light-Driven Growth of Micelles Obtained from in Situ Nanoparticlization of Conjugated Polymers. *J. Polym. Sci. Part Polym. Chem.* **2017**, *55* (18), 3058–3066. https://doi.org/10.1002/pola.28598.

(3) Yoshida, S.; Ejima, H.; Yoshie, N. Tough Elastomers with Superior Self-Recoverability Induced by Bioinspired Multiphase Design. *Adv. Funct. Mater.* **2017**, *27* (30), 1701670. https://doi.org/10.1002/adfm.201701670.

(4) Ishizaka, S.; Nakagawa, S.; Yoshie, N. Computer-Aided Design of Copolymers with Controlled Comonomer Distributions. *Macromolecules* **2023**, *56* (18), 7312–7319. https://doi.org/10.1021/acs.macromol.3c00409.

(5) Ishizaka, S.; Nakagawa, S.; Matsuoka, K.; Yoshie, N. Tough Polymer with a Gradual Spatial Change in the Hydrogen Bond Density Controlled by Simple One-Pot Copolymerization. *Polymer* **2022**, *246*, 124748. https://doi.org/10.1016/j.polymer.2022.124748.

(6) Takagi, H.; Igarashi, N.; Mori, T.; Saijo, S.; Ohta, H.; Nagatani, Y.; Kosuge, T.; Shimizu, N. Upgrade of Small Angle X-Ray Scattering Beamline BL-6A at the Photon Factory. *AIP Conf. Proc.* **2016**, *1741* (1), 030018. https://doi.org/10.1063/1.4952841.

(7) Huang, T. C.; Toraya, H.; Blanton, T. N.; Wu, Y. X-Ray Powder Diffraction Analysis of Silver Behenate, a Possible Low-Angle Diffraction Standard. *J. Appl. Crystallogr.* **1993**, *26* (2), 180–184. https://doi.org/10.1107/S0021889892009762.

(8) Frisch, M. J.; Trucks, G. W.; Schlegel, H. B.; Scuseria, G. E.; Robb, M. A.; Cheeseman, J. R.; Scalmani, G.; Barone, V.; Petersson, G. A.; Nakatsuji, H.; Li, X.; Caricato, M.; Marenich, A. V.; Bloino, J.; Janesko, B. G.; Gomperts, R.; Mennucci, B.; Hratchian, H. P.; Ortiz, J. V.; Izmaylov, A. F.; Sonnenberg, J. L.; Williams; Ding, F.; Lipparini, F.; Egidi, F.; Goings, J.; Peng, B.; Petrone, A.; Henderson, T.; Ranasinghe, D.; Zakrzewski, V. G.; Gao, J.; Rega, N.; Zheng, G.; Liang, W.; Hada, M.; Ehara, M.; Toyota, K.; Fukuda, R.; Hasegawa, J.; Ishida, M.; Nakajima, T.; Honda, Y.; Kitao, O.; Nakai, H.; Vreven, T.; Throssell, K.; Montgomery Jr., J. A.; Peralta, J. E.; Ogliaro, F.; Bearpark, M. J.; Heyd, J. J.; Brothers, E. N.; Kudin, K. N.; Staroverov, V. N.; Keith, T. A.; Kobayashi, R.; Normand, J.; Raghavachari, K.; Rendell, A. P.; Burant, J. C.; Iyengar, S. S.; Tomasi, J.; Cossi, M.; Millam, J. M.; Klene, M.; Adamo, C.; Cammi, R.; Ochterski, J. W.; Martin, R. L.; Morokuma, K.; Farkas, O.; Foresman, J. B.; Fox, D. J. Gaussian 16 Rev. C.01, 2016.